SSC16-III-03

The NASA Optical Communications and Sensor Demonstration Program: Initial Flight Results

Siegfried Janson, Richard Welle, Todd Rose, Darren Rowen, Brian Hardy, Richard Dolphus, Patrick Doyle, Addison Faler, David Chien, Andrew Chin, Geoffrey Maul, Chris Coffman, Stephen D. La Lumondiere, Nicolette I Werner and David Hinkley
The Aerospace Corporation
Mail Stop M2-241, P.O. Box 92957, Los Angeles, CA 90009-2957; 310-336-7420
siegfried.w.janson@aero.org

ABSTRACT

The NASA Optical Communications and Sensors Demonstration program was initiated in 2012 to demonstrate optical communications from orbit at a 5 Mbps rate and demonstrate proximity operations using CubeSats. The original two spacecraft effort became a three spacecraft effort in 2015 with the first "Pathfinder" spacecraft (AeroCube OCSD-A) launched in October, 2015, to be followed by a fully-operational pair of Demonstration CubeSats (AeroCubes OCSD-B and –C) in October, 2016. The Pathfinder was flown without a propulsion system and was meant to test attitude control accuracy and a 6W, two-stage, downlink laser. Initial on-orbit checkout proceeded as planned until a software upload to the attitude control system (ACS) corrupted the boot sequence and rendered the processor inoperable. On-orbit software updates had been routine for AeroCubes for many years. This particular upload was different, and resulted in an ACS software failure. Unfortunately, the laser communications subsystem was controlled by the ACS processor and could not be turned on even to check power levels. OCSD-A is still a functional satellite, but without pointing capability. There are many new subsystems on this pathfinder that are being evaluated. This paper will provide an update on those new subsystems, specifically the OCSD-A star tracker, high-resolution camera, and the software-defined radio. It will also discuss the software error that occurred on OCSD-A, the modifications applied to the OCSD-B and –C to correct this problem, and design and testing of the steam thrusters currently planned for OCSD-B and –C.

HISTORY

The Optical Communication and Sensor Demonstration was funded by NASA's Small Spacecraft Technology Program (SSTP) under the Space Technology Mission Directorate. The original goals were to demonstrate satellite-to-ground laser communications from a CubeSat with a data rate greater than 5 Mbps, to demonstrate proximity operations using two identical spacecraft, and to demonstrate tracking of one spacecraft by the other. This effort evolved in 2015 from a two-CubeSat flight demonstration to a Pathfinder mission launched in October, 2015, to be followed by a two-spacecraft demonstration mission now scheduled for October, 2016. We significantly increased the original 5 Mbps data rate threshold by changing from a 300 mW output direct-drive laser diode to a two-stage 6 W, and finally, a one-stage 2W fiber laser. The two-stage laser was flown on AeroCube-OCSD-A while the one-stage version will fly on AeroCube-OCSD-B and –C. Our potential downlink data rates are now in excess of 200 Mbps. Multiple papers chronicle the evolution of this NASA-sponsored effort.[1,2,3,4]

THE PATHFINDER SPACECRAFT

Figure 1 shows a photograph of AeroCube-OCSD-A, the Pathfinder was launched on Oct. 10 2015. It contained a 6-W output downlink laser, an uplink laser receiver/quadcell, two independent 915 MHz communications transceivers, a GPS receiver, a 3-axis attitude control system designed for better than 0.15^{o} pointing accuracy, a Jenoptik DLEM-SR laser rangefinder,[5] two star trackers, a color camera with 180^{o} field of view, a proximity operations color camera, two deployable solar panels, and a distributed computing system composed of over 20 microprocessors and 3 field-programmable gate arrays (FPGAs). An 8-gigabyte flash RAM memory card was to be used for data storage. The Earth-pointing face is the top face in Fig. 1; this face contains the uplink receiver, the transmitter output window, a medium-gain patch antenna, a sun sensor, a laser retro-reflector, an ultra-wide angle camera, an LED beacon, and our legacy Earth nadir sensor. The locations are shown in the schematic drawing in Figure 2.

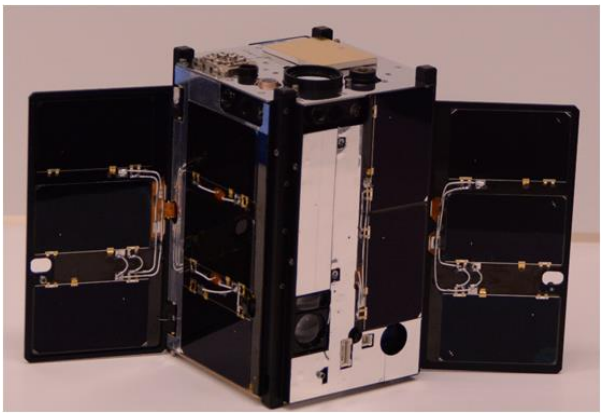

Figure 1. Photograph of the Pathfinder spacecraft with solar wings deployed.

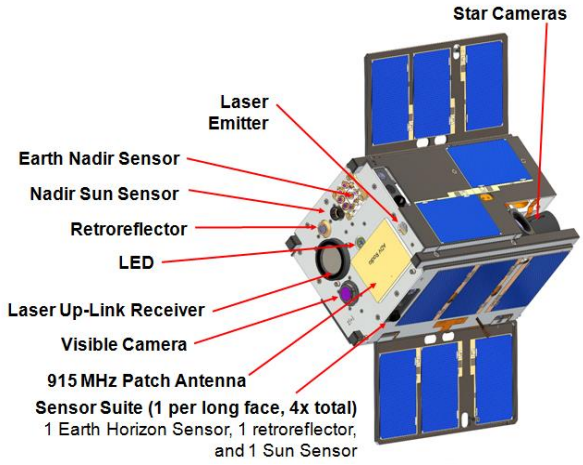

Figure 2. Location of nadir-face components.

Attitude Control System Failure

The Pathfinder (OCSD-A) was added to the program as a risk-reduction flight to test key new systems: an attitude control system with 0.15º pointing accuracy, and a 6W laser downlink. The spacecraft was launched with unfinished software modules since the process for uploading software updates had been previously demonstrated over 350 times across 9 different spacecraft. This time, however, the software upload to the attitude control processor experienced an on-orbit anomaly that rendered the attitude control system inoperative. Unfortunately, the attitude control processor also controlled downlink laser activation for safety reasons, so both the attitude control and laser downlink systems were disabled. In addition, all attitude sensors, actuators, and the laser rangefinder were disabled.

The flight anomaly was traced to a change in processor partitioning, without a change in the uploading sequence. Flight uploads typically occur incrementally over several ground contact periods, and data blocks are uploaded sequentially. In our case, a new processor partitioning scheme required a non-sequential upload; not a sequential one. Between ground contacts, the AeroCube-OCSD-A vehicle executed a regularly scheduled power-cycle, and this power-cycle re-booted the ACS processor into a partially, but not fully, updated program which prevented proper initialization. The power-cycle re-boot was not included in our pre-upload ground simulation, and we ended up with a "bricked" processor; an inert device that would not accept further updates. Unfortunately, this processor handled attitude sensor and actuator data, leaving the spacecraft without active attitude control.

Flight Data

Attitude sensors, including magnetometers, sun sensors, the Earth nadir sensor, and two different rate gyro triads, plus actuators such as the reaction wheels and magnetic torque rods, were tested for basic operation during the initial spacecraft checkout phase. These operated as expected. Uploading of new attitude control software such as the B-dot despin routine occurred next. This is when the attitude control processor became unresponsive. Operational post-failure systems included the power system (new), camera image processing board (new), GPS receiver, a software defined radio transceiver (new), the primary communications transceiver, the command and control system, a distributed temperature monitoring system, two star tracker cameras (new), the wing deployment system (new) and the star tracker baffle deployment system (new). The software defined radio is a redundant radio that offers download rates up to 500 kbps. All of these systems operated as expected, thus validating their design and testing procedures. AeroCube-OCSD-A is power positive, thermally stable, and in daily contact with our ground stations. It has reduced risk for the upcoming AeroCube-OCSD-B&C flights, but not by as much as we had originally planned. Nevertheless, we learned important lessons.

Passive rotation rate damping mechanisms such as Eddy current generation in the aluminum hull and flexing of board stacks, the deployed wings, etc., have slowly despun the spacecraft over weeks and months. This allowed testing of the proximity and star tracker cameras with spacecraft rotation rates below 1 degree per second. Figure 3 shows an image downloaded from the 10-Megapixel proximity camera mounted near the bottom right corner of the right body panel shown in Fig. 1. This image is centered near Quinhagak, Alaska and includes parts of the Togiak and Yukon Delta

Figure 3. Photo of southwest Alaska taken using the Proximity Camera on March 15, 2016.

National Wildlife Refuges. Ground resolution was only 1000' (305 meters) due to the small lens aperture. This was an image of opportunity; the proximity camera happened to pointing at the Earth when we commanded an image acquisition.

Star tracker images were accessible through the camera image processing board, so we were able to download images and process them on the ground to verify star tracker operation. These star trackers enable 0.02° angular determination accuracy that will be needed in the upcoming –-B&C demonstration flights, so this was an important test. We took multiple stellar images before and after wing deployment, which produced a decrease in rotation rate from 0.97°/s to 0.80°/s.

Figure 4 shows part of a processed image in negative form taken on Dec. 2, 2015, before wing deployment. This was about 6 weeks after launch. The large black blobs are stellar tracks while the individual dots are either hot or warm pixels. Hot pixels are much brighter than the median level while warm pixels are only a few counts above the median. Maximum counts per pixel is 255, and the imagers have a 760 x 480 pixel format. About 1450 single dots appear in whole image, which is much larger than the 381 hot pixels measured during ground tests. These hot pixels are indicated by red circles in Fig. 4. Radiation is most likely creating new hot pixels; we will monitor the number of these pixels in each imager as a function of time. No warm pixels were measured during ground tests.

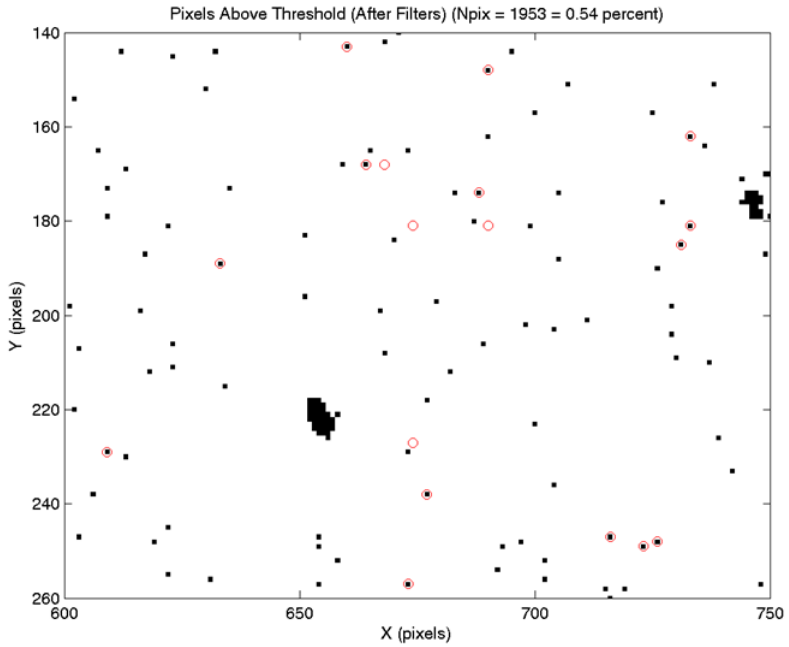

Figure 4. Part of a processed stellar image, in negative form, from one of the star trackers.

Post wing deployment measurements showed that stellar magnitudes down to 4.5 provided reliable targets with a signal-to-noise ratio (SNR) of 3 or better using a 150 millisecond exposure. Stars down to magnitude 5 were detectable at SNR=2, and the on-orbit background noise level was 10 counts per pixel. Note that Fig. 4 shows only 5% of the full image frame. Monte Carlo analyses using 500 random attitudes have shown that 3 or more stars, the number needed for a 3-axis attitude fix, are available with SNR>=3 at least 55% of the time at the angular rotation rate of 0.8°/s. With a lower SNR of 2, that increases to 86% of the time. At lower rotation rates, dimmer stars become visible. At a 0.1°/s rate, our star tracker can see 3 or more stars with an SNR>=3 98% of the time when sunlight and Earthshine do not interfere. Even higher levels of availability are possible using both star trackers since they observe different parts of the sky. Overall, our star trackers have proven that they can provide the needed attitude determination accuracy for the upcoming AeroCube-OCSD-B&C flight demonstrations.

THE FLIGHT DEMONSTRATION

AeroCube-OCSD-B & -C demonstration spacecraft are currently scheduled to fly in late October, 2016, on a Falcon-9 launch vehicle, and deployed by the SHERPA multi-payload adapter. The planned orbit is sun-synchronous at 720-km altitude. The laser downlink was changed from that in AeroCube-OCSD-A to be more reliable and easier to integrate, and a steam propulsion module will be in each vehicle to facilitate proximity operations between the two spacecraft. Due to extra launch delays that were added during the last six months, we were able to implement a number of changes to both spacecraft to fix issues that were observed in the Pathfinder flight. Most notably, we implemented software changes and new procedures for on-orbit software uploads.

Downlink Laser Modifications

Several design changes to the AeroCube-OCSD-A laser downlink transmitter were implemented for the -B and –C demonstrators. Most notable was the reduction of divergence from ~0.35° full-width half-maximum (FWHM) to ~0.15° and ~0.05° to compliment expected improvements in AeroCube pointing capability. This enabled us to downscale the transmitter output from 6-to-10 W to 2-to-4 W. Note that the two demonstrator spacecraft will have different beam divergences; the 0.15° beam will be easier to aim at the ground station and can provide the baseline data rate, while the 0.05° beam will enable demonstration of higher data rates due to increased photon flux on target. The baseline 2 W laser is now a lower-risk single-stage Ytterbium fiber amplifier design compared to the previous two-stage configuration. The second stage pump laser, the second stage gain fiber, an optical isolator, and associated power and control circuitry for the second pump laser were no longer required. Comparatively, the new laser transmitter module occupies the same 10x10 cm^2 cross-sectional footprint but is approximately 2 cm in height which is a 20% reduction. Further, the weight of the transmitter was reduced from 615 to 360 g. Photos of the AeroCube-OCSD-A and the new –B & -C laser modules are shown in Figures 5 and 6, respectively.

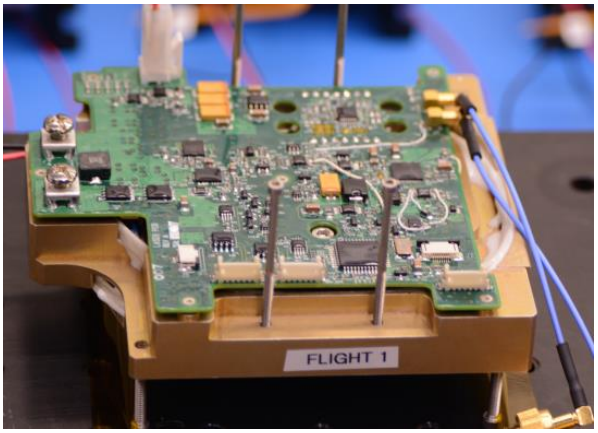

Figure 5. Downlink laser in the Pathfinder (AeroCube-OCSD-A).

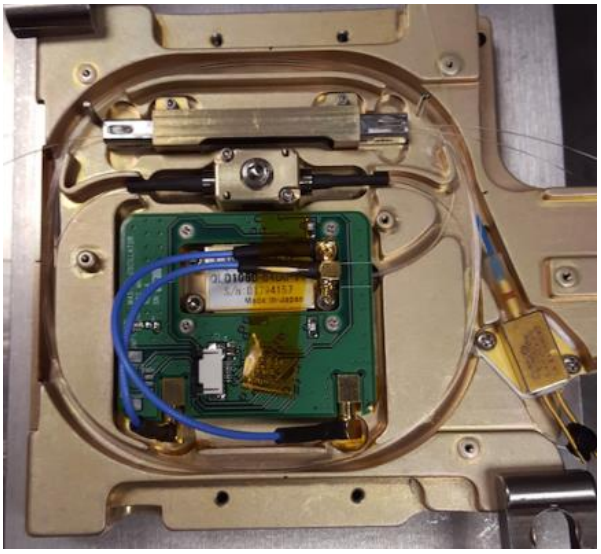

Figure 6. Downlink laser in the Demonstrators (AeroCube-OCSD-B and -C).

The overall wall-plug efficiency of the single-stage laser is ~20%. A significant effort was made to impedance match the data drive circuitry to the commercial seed DFB laser diode laser which is housed

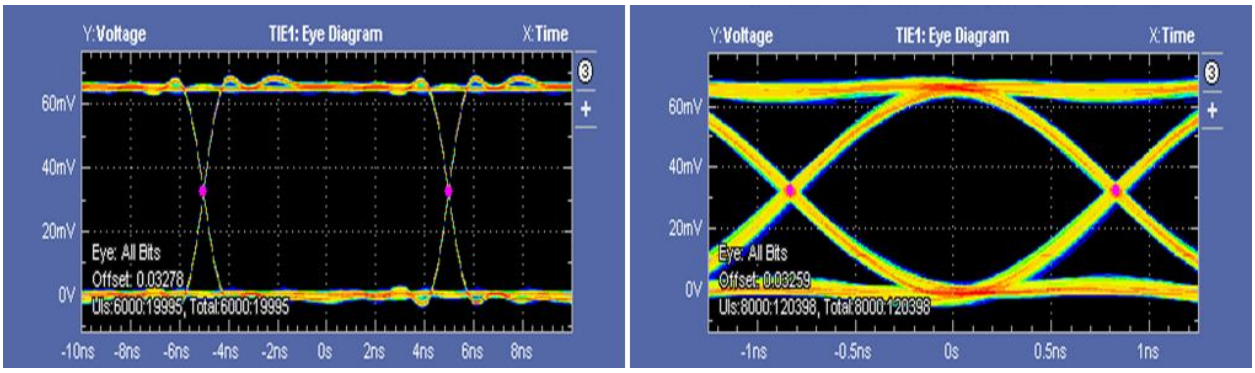

Figure 7. Eye diagrams for the new laser transmitter at 100 Mbps (left) and at 622 Mbps (right).

in a 14-pin butterfly package. This effort enabled us to achieve clean direct modulation up to 800 Mbps. Under the previous un-optimized configuration, distortion became notable for data rates exceeding 300 Mbps. The results of the electrical rework can be seen in the eye-diagrams presented in Figure 7. As before, the laser wavelength is held fixed at 1064 nm by a thermoelectric cooler internal to the seed laser package.

Propulsion Module Modifications

Our single-thruster propulsion module uses water as propellant, and ejects water vapor (steam) into space. We chose water because it has a vapor pressure below 1 atmosphere (no pressure vessels), provides a quite respectable specific impulse of about 90 s, and is one of the easiest propellants to meet flight safety requirements. The basic structure is fabricated in plastic using additive manufacturing.

Figure 8 shows a photograph of the current design. The nozzle is hidden on the bottom surface and shoots downward. Improvements to the thruster module originally slated for the Pathfinder mission include:

1. Extra heating coils to maintain a 40 ^{o}C operating temperature.
2. Reduced propellant tank thickness to provide room for extra heaters and wiring,
3. Ribs added to walls to increase wall strength,
4. Conformal coating of internal sensors to eliminate corrosion,
5. More robust mounting of external sensors to reduce wire breakage,
6. Resizing of pressure sensor mounting holes to eliminate propellant leakage, and
7. Reduced propellant fills.

The need for extra heating coils became apparent during early testing. We needed a more uniform temperature distribution, so external heating coils and a reflective thermal blanket were added to the design. To fit within the same volume, the tank was redesigned to have thinner walls, but with internal ribs to get back tank stiffness. We also added a thermistor to the nozzle for monitoring temperature, and this required several iterations to produce a mechanically robust design.

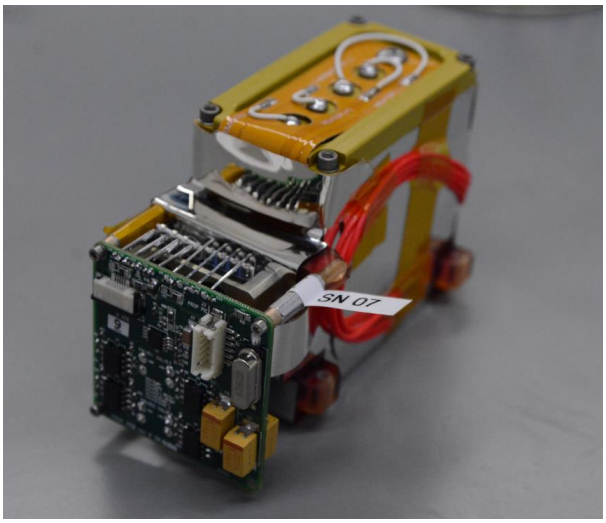

Figure 8. Photograph of the AeroCube-OCSD-B &-C propulsion module.

The corrosion and propellant leakage issues were identified after months of sitting dormant in the laboratory. This required changing some sensors, using conformal coating on internal temperature sensors, and improving the propellant tank openings to properly seal around the pressure sensor.

Propellant fill volume became an issue during extended vacuum testing. Sometimes an ice ball would form in front of the nozzle, but only during the first or second firing after refilling the module. This was traced to liquid water, and not steam, being ejected from the nozzle. Normally, our propellant management device

(a sponge) holds the liquid water, but overfilling the tank provides free liquid water than can be forcefully ejected. Our modules are also filled with water in the open laboratory at 1 atmosphere pressure. This results in a ~15 psi pressure in the propellant tank prior to first firing in vacuum, rather than the typical ~1 psi vapor pressure at 40 ºC. The solution was to carefully measure the liquid propellant fill (26.0 cc) so as to not exceed the storage capacity of the sponge, to carefully vent the propellant tank during the vacuum pump down, and to deliver propulsion modules with reduced internal pressure.

We tested thrust generation in the laboratory by mounting the thruster module on a sensitive electronic balance (scale) with the nozzle pointing up. The whole system, except for electronic balance display, was put in a vacuum chamber with feedthroughs carrying the scale data output lines, the RS-232 thruster control lines, and the power plus ground lines for both the thruster and the scale. We operated the thruster while monitoring the scale output. The baseline level is the weight of the thruster module plus assorted wires and connectors, as measured by a load cell in the scale. Temporary increases in force are due to thrust. Figure 9 show the measured temporal response of our thruster at 40 ºC with pulse widths of 250 and 1000 milliseconds. Maximum thrust is 3 mN, and the impulse bit at 250 ms is 0.6 mN-s.

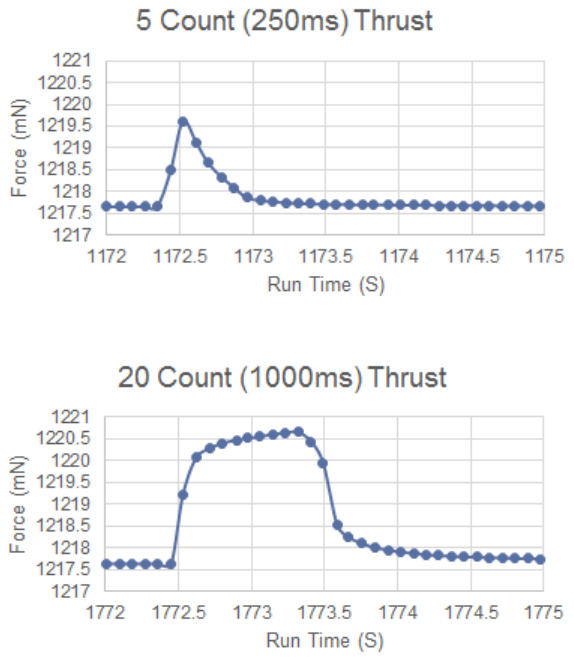

Figure 9. Thrust measurements for 250 and 1000 ms pulse widths.

Software Upload Modifications

Figure 10 shows an example memory map for the 16-bit attitude control processors on AeroCube-6 and AeroCube-OCSD-A (AC-7A). In both cases, the Boot Library references a set of Boot-initiated variables that are located elsewhere. Our legacy code had the Initialization and Boot Library fields immediately after the initial Reset/GoTo instruction, with the Boot-initiated variable field located at higher addresses. The AeroCube-OCSD-7A code had Patching Functions immediately following the Reset/GoTo instruction, with the Boot-Initiated Variables being located between the Patching Functions and the Initialization/Boot Library. In addition, ACS code was inserted between these two memory blocks. The OCSD-7A flight failure occurred because of a spacecraft reboot that occurred after the Boot-initialized Variables block was uploaded, but before the Initialization / Boot Library block could be updated. An entire processor update may not occur during a single ground station pass. When the processor "woke" up after the reboot that occurred between ground station passes, the Reset GoTo instruction sent it to the section of Initialization code that diverged in partitioning from legacy vehicles. The Initialization code then attempted to access an incompatible initialization table in the Boot-initialized Variables block, thereby causing the ACS processor to become unresponsive.

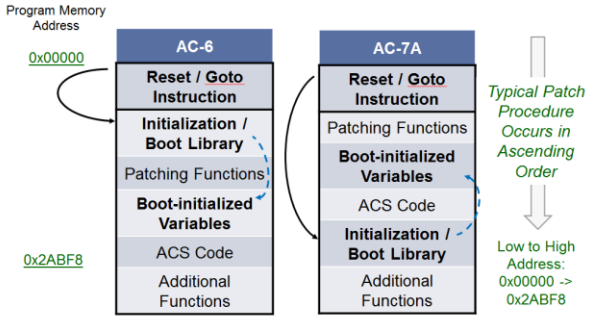

Figure 10. Example memory maps for legacy (AeroCube-6) and OCSD-A (AC-7A) ACS processors.

We redesigned the processor code to separate the "patch" (software update) function from the main application. Figure 11 shows an example of this. The Bootloader code and variables immediately follow the Reset/GoTo instruction, and the main code follows after. On Reset, the ACS processor enters the Bootloader section, but cannot execute the main application unless commanded to do so. This enables patching of the main application, even if the main application fails. It just requires a processor reboot or power cycle. There is no plan to modify the bootloader

code in flight, but in the event that an update is required, it is theoretically possible to load a redundant bootloader into the main program area. This would permit an update to the primary bootloader, but has not yet been demonstrated.

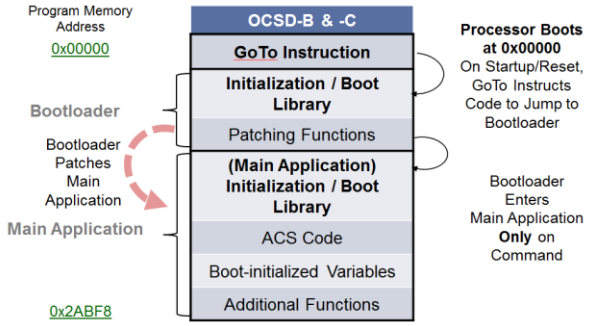

Figure 11. Redesign of the ACS processor program memory map.

CONCLUSION

AeroCube-OCSD-A, our Pathfinder spacecraft, lost attitude control capability due to an unexpected anomaly in our software uploading process. This has been corrected for the flight Demonstration (AeroCube-OCSD-B & -C) and future spacecraft. While the attitude control system, laser downlink, and laser rangefinder could not be tested on-orbit, OCSD-A has provided valuable flight data on other new systems and components like the software-defined radio, the power system, and the star trackers. We redesigned the laser downlink transmitter for the Demonstration and future spacecraft to be simpler, less massive, smaller, and more reliable than the Pathfinder version. In addition, we made improvements to the steam propulsion module that will be required for the proximity operations demonstration using the OCSD-B & -C spacecraft. Both spacecraft have been assembled, tested, and are awaiting integration into the launch vehicle. Figure 12 shows the completed AeroCube-OCSD-C spacecraft getting weighed in flight delivery configuration. The zenith-pointing face is up, and it has a mass of 2.31 kg. Not surprisingly, AeroCube-OCSD-B has the same mass.

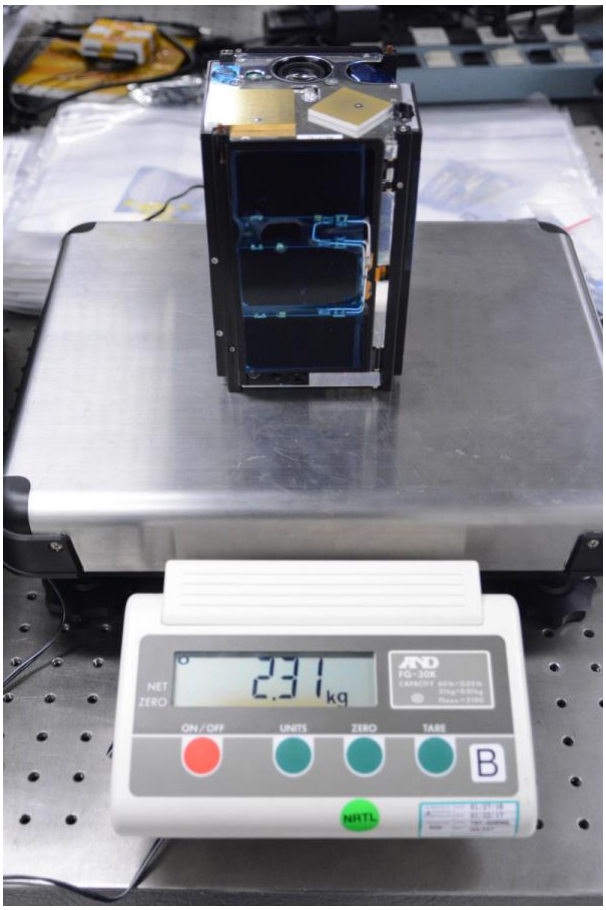

Figure 12. AeroCube-OCSD-C getting weighed.

References

1. Janson, S.W., and Welle, R.P., "The NASA Optical Communication and Sensor Demonstration Program," paper SSC13-II-1, AIAA/USU Small Satellite Conference, Logan, Utah, August 10-15, 2013.

2. Janson, Siegfried W., and Welle, Richard P., "The NASA Optical Communication and Sensor Demonstration Program: An Update," paper SSC14-VI-1, 28th AIAA/USU Small Satellite Conference, Logan, Utah, August, 2014.

3. Rose, T.S., Janson, S.W., LaLumondiere, S., Werner, N., Hinkley, D.A., Rowen, D.W., Maul, G., Fields, R.A., and Welle, R.P., "LEO to Ground Optical Communications from a Small Satellite Platform," *Proc. SPIE 9354*, Free Space Laser Communication and Atmospheric Propagation XXVII, 935401, March, 2015.

4. Janson, Siegfried W., Welle, Richard P., Rose, Todd S., Rowen, Darren W., Hinkley, David A., Hardy, Brian S., La Lumondiere, Stephan D., Maul, Geoffrey A., and Werner, Nicolette I., "The NASA Optical Communication and Sensors Demonstration Program: Preflight Update," paper SSC15-III-1, 29th Annual AIAA/USU Conference on Small Satellites, Logan, Utah, August 2015.

5. Jenoptik, DLEM-SR Datasheet, Jenoptik Defense and Civil Systems, Jena, Germany, URL: http://www.jenoptik.com/cms/products.nsf/0/645924FE73AE3A1EC125790A0037F7ED/$File/dlem_sr_en_web.pdf?Open , June 2014.